TD-DFT Modeling of the Circular Dichroism for a Tryptophan Zipper Peptide with Coupled Aromatic Residues

ANJAN ROY,[1] PETR BOUŘ,[2] AND TIMOTHY A. KEIDERLING[1]*
[1]*Department of Chemistry, University of Illinois at Chicago, Chicago, Illinois*
[2]*Institute of Organic Chemistry and Biochemistry, Academy of Sciences, Prague, Czech Republic*

Contribution to the Special Thematic Project "Advances in Chiroptical Methods"

ABSTRACT In this work, time dependent density functional theory (TD-DFT) is used to provide a reliable basis for interpretation of the electronic spectra of coupled tryptophan (Trp) residues, particularly those in a model Trpzip β-hairpin peptide. Pairs of isolated indoles form chiral coupled chromophores whose computed electronic ultraviolet circular dichroism (CD) is in excellent agreement with observed transition wavelengths and intensities. The calculations were compared to experimental data for pairwise coupling in mutant Trpzip peptides that are recently available. A study of variation of the basis set, geometry optimization, and the solvent environment on the spectra showed limited impact on bandshapes. An alternative simplified computational scheme, dependent on the transition dipole coupling (TDC) mechanism, is shown to give a representation of qualitative aspects of the intense CD for the ^{1}B bands at 228 and 213 nm. The results confirm the origin of the Trpzip diagnostic CD as primarily a dipolar interaction between Trp sidechains, and show that quantum computations of electronic CD can provide a reliable basis for interpretation of these chirally coupled aromatic spectral phenomena. *Chirality 21:S163–S171, 2009.*

KEY WORDS: tryptophan; indole; Trpzip β-hairpin peptides; circular dichroism; TD-DFT

INTRODUCTION

Tryptophan (Trp) is a chiral amino acid with an aromatic side-chain whose low lying electronic states are of critical value for fluorescence studies of proteins and peptides. Additionally, absorbance spectra of these states provide a useful marker for concentration determination. Consequently the electronic structure and excited state properties of indole have long been of wide interest.

The associated electronic circular dichroism (CD) of aromatic electronic transitions in an isolated amino acid is relatively weak due to the local planarity of the indole chromophore. On the other hand, in folded proteins or other stereochemically constrained environments, these Trp transitions yield useful, easily measured CD, typically detected at 280 nm, whose presence or absence correlates with tertiary structure in the folded protein. If two or more Trp are in the protein sequence and have a fixed geometry, a particularly strong CD may occur, as their transitions can couple and develop an exciton chirality whose distinctive shape and sign pattern could be used to determine the relative stereochemistry of the chromophores.

Recent studies of designed β-hairpin peptide structures, that are stabilized by hydrophobic interactions of various residues, have highlighted the special role of Trp.[1–3] In particular, in a set of peptides denoted as tryptophan zippers (Trpzip) the Trp-Trp exciton coupled CD, which yields an intense couplet shape in the far-ultraviolet (UV), was used to follow temperature induced unfolding of the hairpins.[1,4–6] The dominant bands seen in these peptides form a positive couplet (−/+ with increasing wavelength) that does not correspond to Trp bands often used to monitor protein tertiary structure (at ∼280 nm) but rather to higher energy transitions at 227(+) and 213(−) nm. Because of the strong coupling of these Trp chromophores in the far UV region, the CD arising from their $\pi-\pi^*$ transitions completely obscures the weaker (∼5 times) amide CD bands which are traditionally used for secondary structure analysis. The side-chain CD almost disappears for these peptides when they unfold at higher temperatures. The lower energy transition, which corresponds to that used in protein near-UV CD, can be detected as a single signed CD band, whose temperature dependence tracks that of the couplet.[6]

Additional Supporting Information may be found in the online version of this article

Contract grant sponsor: National Science Foundation; Contract grant number: CHE07-18543.
Contract grant sponsor: Czech Republic; Contract grant number: 202/07/0732.
Contract grant sponsor: Czech Academy of Sciences; Contract grant numbers: A400550702, M200550902.
*Correspondence to: Timothy A. Keiderling, Department of Chemistry, University of Illinois at Chicago, Chicago, Illinois. E-mail: tak@uic.edu
Received for publication 20 May 2009; Accepted 4 August 2009
DOI: 10.1002/chir.20792
Published online 6 November 2009 in Wiley InterScience (www.interscience.wiley.com).

We have studied several mutants of these Trpzip peptides with different residues substituted for the Trps in various pairs at cross-stranded positions.[6,7] These have shown that IR spectra can be used to follow secondary structure (β strand) change in these peptides, while CD and fluorescence can follow tertiary structure (Trp-Trp interaction) change. Because of the central role of Trp CD in these model systems as well as for proteins overall, it is important to develop a better understanding of their electronic spectra. In this article, we particularly address the CD that can arise from stereochemical interactions of electronic (UV) excitations on two or more Trp residues, with a specific application of modeling one Trpzip system.

Recently, complete active space self consistent field (CASSCF) calculations have been used to successfully model excited state calculations; however, their high computational cost favors their use for smaller molecular systems.[8] The advent of widely accessible packages for time dependent density functional theory (TD-DFT) method computations has allowed quantum mechanical calculation of properties of excited states with moderately sized computers at relatively low computational expense. Recent research on the electronic spectra of tryptophan using TD-DFT[8,9] has centered on the near UV transitions, i.e. those localized at the indole ring which are denoted as ^1L_a and ^1L_b in Platt's notation.[10] These are the well studied $\pi-\pi^*$ excitations from ground to the low lying excited (singlet) states and, according to Kasha's rule, are the source of the fluorescence emitting states for tryptophan.[8,11] There has been considerable debate over the relative ordering of these states and their detailed properties,[8,12,13] but for our specific CD analyzes, such issues are not critical, thus we will not comment on them directly. In this work, we instead focus on the more intense $\pi-\pi^*$ transitions in the 190–230 nm region (^{1}B states), which for Trpzip peptides dominate the far-UV CD spectrum and absorbance. In Trpzip, aromatic residues are designed to interact and thus occur in cross-stranded pairs.

The coupled oscillator (CO) model[14] can also help develop a qualitative understanding of the CD of these intense transitions, which depends on rotational strengths arising from dipole orientation and splitting due to the dipolar interaction. Here we go beyond such a transition dipole coupling (TDC) based method by using ab initio approaches based on the TD-DFT methodology. To our knowledge, this is the first time TD-DFT has been used to study the ECD of coupled tryptophans, although one of these computational results was reported in a previous article to explain the source of the UV CD in a Trpzip hairpin.[6] TD-DFT has been previously used for computing excited states of indoles[8] and has been criticized with regard to its application for larger ring systems,[12,15] however, our comparison of theoretical to experimental results for the ^{1}B transitions in the Trp side-chain indole chromophore are satisfactory, and those of the ^{1}L are also acceptable, as will be shown.

COMPUTATIONAL METHODS

TD-DFT calculations with a reasonable basis set for the excited states of a complete Trpzip2 molecule (209 atoms), the most stable small β hairpin model available,[1] would be computationally expensive. Fortunately, because most of the observed electronic CD arises from the Trp side-chain and not the amide backbone, we could restrict ourselves to a series of excited state calculations on isolated indoles. For computing CD, chirality develops from the coupled indole models whose relative geometries were fixed to correspond to those of the Trp side-chains in Trpzip2. These local geometries are functionally the same in Trpzip1 and in the mutant structures we have prepared with only two Trp residues (see Fig. 1).[1,4–6] Transition energies and intensities were computed for isolated indole rings with different basis sets, and also for indoles with methyl substituents which represent a connection to the peptide backbone, the β methylene carbon of Trp. The hybrid functional, B3LYP, was chosen because of previous successes using it for these excited states.[16] To model the effect of solvation, we used the polarized continuum model (PCM),[17] which considers the solute to be in a dielectric cavity whose electrostatic potential is derived from the dielectric of the solvent, in our case water (ε_r = 78.39). All computations used either Gaussian 03 Rev D.02[18] or Turbomole ver. 5.10[19] quantum chemical packages.

The same kinds of B3LYP TD-DFT electronic excitation computations, but including CD, were repeated using a 6-31++G** basis set for dimers (and 6-31G** for tetramers) of indole rings that were constrained to selected relative orientations. These model the conformations

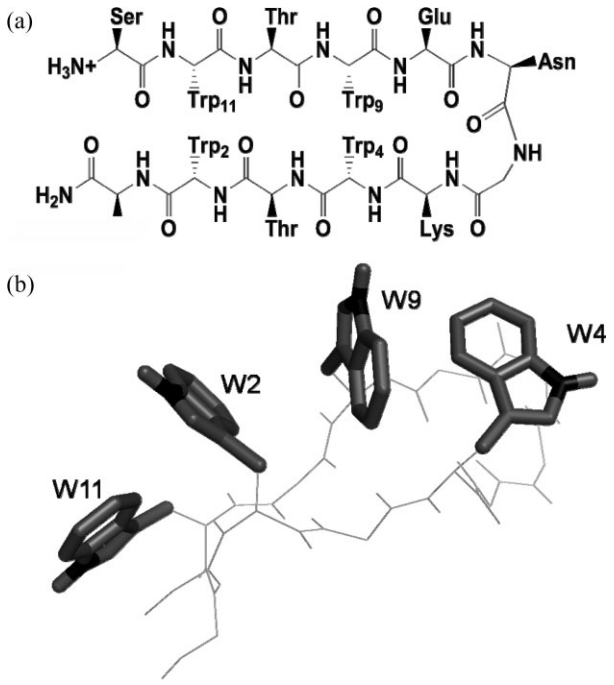

Fig. 1. (**a**) The Trpzip2 peptide indicating the sequential positions of the four Tryptophans involved in the study (2, 4, 9 and 11, top), and (**b**) its three-dimensional representation showing the relative orientations of the Trps (PDB ID: 1LE1[3]).

TABLE 1. Comparison of transition energies and oscillator strengths for indole and 3-methyl indole calculated using various geometries and basis sets

Computational model	Basis set	S_1E (eV)	λ (nm)	f[a]	S_2E (eV)	λ(nm)	f[a]	S_3E (eV)	λ (nm)	f[a]	S_4[b]E (eV)	λ (nm)	f[a]
Indole													
NMR[c]	6–31G**	4.73	262	0.05	5.02	247	0.02	6.35	198	0.16	6.35	195	0.56
vac[d]	6–31G**	4.88	254	0.06	5.00	248	0.04	6.23	199	0.32	6.55	189	0.36
vac[d]	6–31G**++	4.58	271	0.06	4.90	253	0.02	6.00	207	0.77	–	–	–
PCM[e]	6–31G**++	4.47	277	0.08	4.88	254	0.02	5.76	215	0.90	6.45	193	0.22
3MI													
NMR[b]	6–31G**	4.54	273	0.05	4.96	250	0.01	6.12	203	0.62	6.80	182	0.17
vac[d]	6–31G**	4.73	262	0.06	4.95	250	0.02	6.10	203	0.43	–	–	–
vac[d]	6–31G**++	4.53	274	0.07	4.80	258	0.02	5.78	214	0.48	6.14	202	0.14
PCM[e]	6–31G**++	4.42	281	0.10	4.78	259	0.03	5.62	220	0.81	6.08	204	0.13

[a]Dimensionless oscillator strength.
[b]S_4 transitions were not uniquely assigned due to their overlap.
[c]Indole and 3MI NMR structure, in vacuum without geometry optimization.
[d]Geometry optimized in vacuum.
[e]Geometry optimized using implicit solvation with water via the PCM.

found for the Trp side-chains in the NMR-determined structure of a Trpzip2,[3] which we have subsequently confirmed to be the same by NMR structure determination for mutated Trpzip2's that have only one pair of interacting Trps.[4,6] The rotational strengths were calculated with the dipole-velocity gauge formulation. To compare theory with experimental CD of the β hairpins, Gaussian functions with a full width at half maximum (FWHM) of 20 nm were scaled to each of the calculated rotational strengths, which when summed approximated the experimental band shapes. Experimental CD spectra, measured in our laboratory, are given in detail elsewhere in the literature,[4–6] and results from those studies will be used here for comparison. Experimental absorbance is more difficult to determine due to overlap of Trp transitions with those of other groups. Thus the computationally more reliable value of $\Delta A/A = \Delta\varepsilon/\varepsilon = 4R/D$ (ratio of rotational, R, and dipole, D, strengths of a single transition) is not available for comparison, which restricts quantitative analyzes of these computations in terms of experimental values.

To estimate the role of the dipolar coupling, the generalized transition dipole (coupled oscillator) model (TDC-CO) was used to compute dimer and tetramer CD employing ab initio computed monomer transition dipoles ($\boldsymbol{\mu}_i$).[20,21] In this method, the interaction Hamiltonian containing only the dipole–dipole interactions is diagonalized. From the eigenvectors [c_{Ei}] dipolar (D) and rotational (R) strengths are obtained for each excited state (E) as

$$\langle D\rangle = \sum_i c_{Ei}^2 \mu_i^2 + 2\sum_{i<j} c_{Ei}c_{Ej}\boldsymbol{\mu}_i \cdot \boldsymbol{\mu}_j,$$

$$\langle R\rangle = -\frac{\omega}{2}\sum_{i<j} c_{Ei}c_{Ej}\mathbf{r}_{ij} \cdot \boldsymbol{\mu}_j \times \boldsymbol{\mu}_i,$$

where ω is the angular frequency of the light, and $\mathbf{r}_{ij}$ the position vector of dipoles i and j.

The input electric transition dipole moments were obtained from the TD-DFT (B3LYP/6-311++G**) computation (see Supporting Information Table S3). Intrinsic magnetic moments were ignored; instead, the electric dipoles were placed close to the molecular center (the 4-atom average) where the magnetic moments (origin dependent) adopt small values. Electric dipoles computed by the velocity formalism were used. Interactions between all possible (20 lowest-energy) Trp transitions were considered, including the states polarized perpendicular to the tryptophan plane. Using NMR structures,[1,6] planes passing through the ring atoms were constructed and the angles between these were subsequently calculated for analysis of the relative geometries.

The adopted TDC-CO model is similar to that used previously in Matrix model calculations by Rogers and Hirst,[22] where fewer tryptophan transitions (calculated at the CASSCF level) were used, but their model Hamiltonian included point charge interactions with the peptide chains. Previously, a TDC-CO approach was used with semiempirical parameters by Grishina and Woody to simulate protein CD.[14]

RESULTS

Single Indole

Geometry optimizations for indole and 3-methyl indole (3MI) were performed starting from a geometry derived from one Trp side-chain taken from the Trpzip2 NMR structure and energy minimizing the indole and related 3MI structures using the B3LYP/6-31++G** level of theory. The agreement between the experimental and calculated geometries was good, e.g., with less than 0.03 Å difference in C8-C9 bond length (similar for N1-C8). The optimized 3MI structure in vacuum obtained with B3LYP/6-31G** is given in the Supporting Information Table S1. TD-DFT calculations were then performed on both the geometry optimized and original structures, which proved to have qualitatively similar transition energies and intensities, the two parameters important for the interpretation of our experiments. Indole and 3MI have a plane of sym-

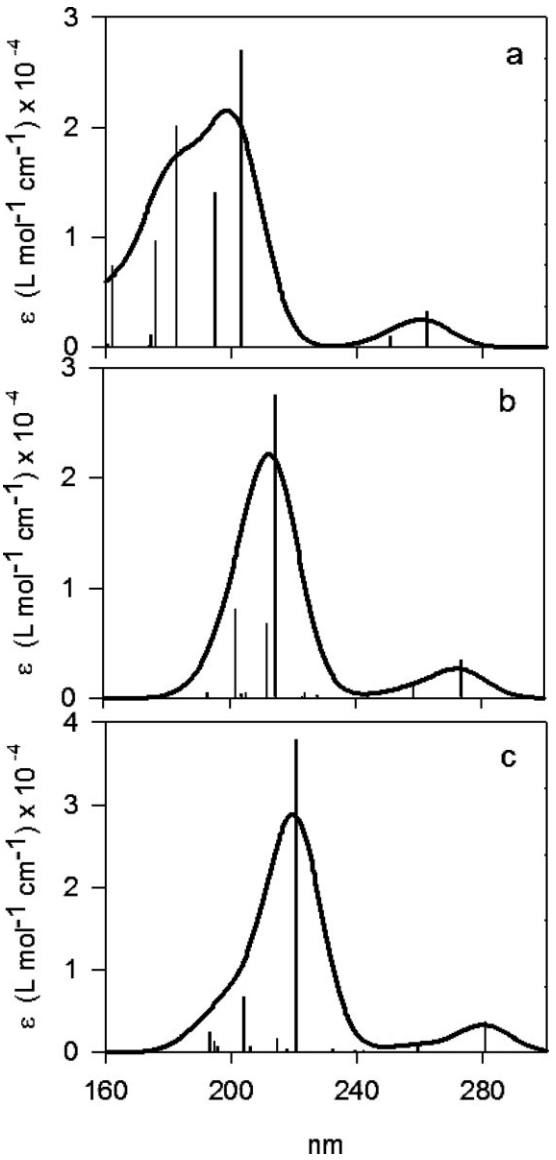

Fig. 2. Calculated UV-absorbance spectra for 3 methyl indole (**a**) in vacuum with a polarized basis set, 6-31G**, (**b**) in vacuum with a diffuse basis set, 6-31++G**, and (**c**) using a PCM model for water with a diffuse basis set, 6-31++G**. Vertical lines represent dipole strengths and solid curves the Gaussian convolutions of calculated bands using FWHM = 20 nm. Note that use of the diffuse basis set adds weak transitions between the ^{1}L and ^{1}B transitions and simplifies the ^{1}B (200–220 nm) region to a few (2 or 3) intense transitions. Diffuse basis functions and PCM solvent models shift transitions down in energy, thus providing a better match to experiment.

metry and therefore have no rotational strength in isolation (no CD). We analyzed their computed oscillator strengths and energies as a test of our basis set selection and computational methods and to gain some insight into the most intense, lowest lying transitions observed in our various indole calculations, as summarized in Table 1 and illustrated in Figure 2.

The unsubstituted indole ring is computed to have four relatively intense transitions in the UV, S_1-S_4, where S_1-S_4 indicate the four lower energy, intense excitations from the ground (S_0) state. S_1 and S_2, the near-UV $\pi-\pi^*$ transitions, are calculated to be at 271 nm and 253 nm with the B3LYP/6-31++G** level of theory. Based on previous literature[13] and calculated dipole strengths, we attribute the 271 nm transition to the ^1L_a and 253 nm to the ^1L_b transition. Additionally, there is one strong $\pi-\pi^*$ transition, S_3, computed near 200 nm, which is >10 times stronger (oscillator strength, f = 0.76) than the ^1L transitions (f = 0.056) and can be assigned to the ^1B_b transition. Some weak transitions are also computed in this range and their number and distribution vary strongly with basis set. Several moderately strong transitions higher in energy than S_3 are seen with the polarized basis, 6-31G**, and they might be designated S_4, which may be the ^1B_a transition. With diffuse functions added, as 6-31++G**, there are fewer of these intense, computed transitions, but the remaining ones are quite mixed in character and correspond to the excitations from the HOMO, HOMO-1 to the higher lying LUMO, LUMO+1 and LUMO+2.[23] This means the S_4 transition is not well characterized and will be consequently of less use in our analyses.

Addition of a methyl group on position 3 of the indole, 3MI, ring shifts the ^1L_a and ^1L_b transitions down in energy and closer together for the 6-31++G** basis set (Fig. 2b); but they remain further apart for smaller basis set calculations (Fig. 2a). The S_3, ^1B_b, shifted down from indole to 3MI (>0.1 eV) and shifts even more with diffuse functions

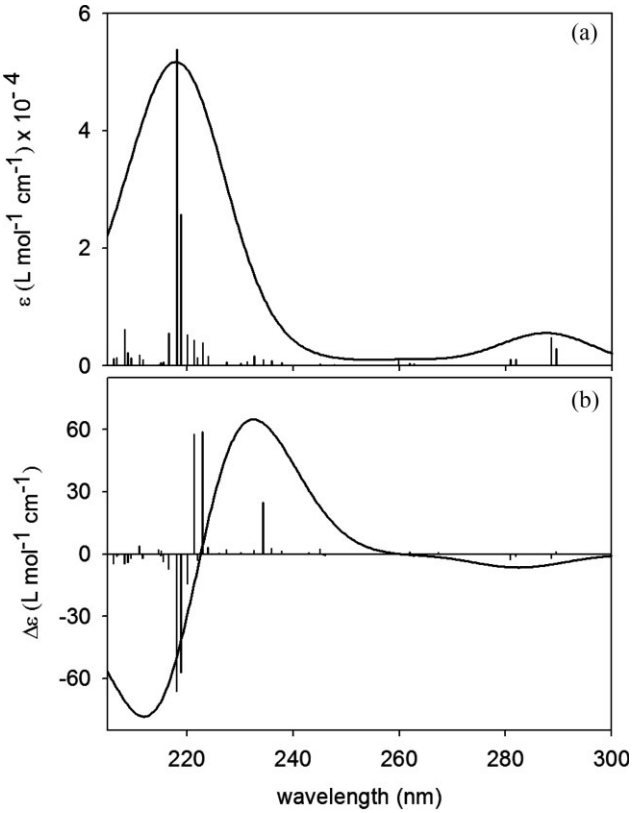

Fig. 3. UV absorption (top, **a**) and CD (bottom, **b**) spectra computed for the two indole pair of W2W11: vertical lines show the TD-DFT B3LYP/6-31++G** computed dipole strengths (top) and rotational strengths (bottom), the solid lines were obtained as the sum of Gaussian components scaled to these strengths (FWHM = 20 nm).

(0.2–0.3 eV), when using 6-31++G**. Computation of the spectra for solvated indole or 3MI, using the PCM model and water parameters, red shifts the entire UV spectrum, as expected (Fig. 2c). The ^1L_a transition and the far-UV ^1B_b transitions show large bathochromic shifts of ~6–8 nm (>0.1 eV), but the ^1L_b transition transitions are much less affected, which is expected since the ^1L_a and ^1B states have larger dipole moments than the ^1L_b state[8] and are stabilized by the dielectric environment imposed by the PCM model.

The geometry change has some impact on the ^1L_a and ^1B transitions but less on ^1L_b, and the diffuse basis set, 6-31++G**, has a substantial effect on all the transitions, as does PCM. With diffuse functions, the transitions shift down in energy, by 0.25–0.3 eV, and become ~50% more intense, thereby enhancing dipole coupling. These behaviors with solvation and values for the transition energies are in good agreement with those found earlier.[8,12]

Two Coupled Indoles Models

Figure 1b shows a schematic representation of the Trpzip2 peptide with emphasis on the relative Trp geometries, as determined from its NMR structure. The Trps interact to stabilize the hairpin structure by forming a hydrophobic face on one side of the folded hairpin. Consideration of only the side-chains was used to model relative interaction geometries for two and four Trp residues. Two 3MI molecules were fixed in space with relative geometries matching those obtained from the Trpzip2 NMR structure by selecting pairs of cross-stranded interacting Trp side-chains. Extending this procedure, using the full Trpzip2 NMR structure (Fig. 1), provides the opportunity to create three combinations with two Trps, W2W11, W4W9, W2W9, that are designated as W(a)W(b), where a and b are the original Trp positions in Trpzip2. A fourth possibility, W4W11, corresponds to the far separated pair of residues which are effectively not coupled, but its spectral parameters were computed for reference. For example, the structural parameters of the W2W11 dimer, as taken from the NMR structure[3] and used for the TD-DFT spectral simulations, are given in the Supporting Information Table S2.

TD-DFT calculations of the coupled excited states, UV absorbance and CD spectra were performed at the B3LYP/6-31++G**/PCM level on the NMR structures without added optimizations since the monomer results (see above) showed a high level of agreement with the NMR structures. Since two planar rings can interact to form chiral pairs of chromophores, their computed CD is nonzero. The Trp side-chains in the three examples studied were separated by 6.8–7.5 Å (measured between C9 positions). In the case of W4W11 the tryptophans were ~17 Å apart and, due to this long distance, did not couple strongly or show significant CD. The computed dipole and rotational strengths are plotted as vertical lines and the envelop corresponding to the overlap of the broadened components as the absorbance and CD spectrum, Figure 3a and 3b, respectively, for the specific case of W2W11. The basic features of most interest in the coupled CD spectrum are the positive couplet computed in the 190–230 nm region and

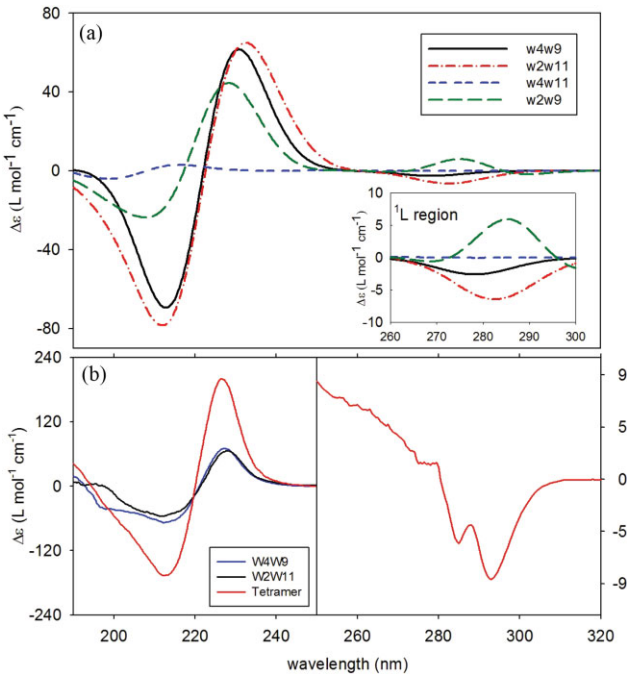

Fig. 4. Top: **(a)** Calculated CD spectra for the selected pairs of indoles: W4W9 (solid), W2W1 (dot-dash), W2W9 (long dash), and W4W11 (short dash), plotted as the sum of components with FWHM = 20 nm, computed at B3LYP/6-31++G**/PCM level (W4W11 at B3LYP/6-31G**). The inset shows a magnified view of the ^1L region. Bottom: **(b)** Experimental far UV CD spectra for trpzip1 (green dash) and Tyr substituted mutants containing two only Trps, data are replotted from Takekiyo et al.[4] (note scale difference), and (c) for the near UV of Trpzip2, replotted from Huang et al.[5] Note scale difference between (b) and (c). [Color figure can be viewed in the online issue, which is available at www.interscience.wiley.com.]

the low energy negative peak in the 260–300 nm region. Coupling of the ^1B_b transitions on each Trp is the important contribution for the former, intense couplet. In the latter case, the ^1L_a and ^1L_b transitions on both contribute.

The W2W11 and W4W9 cases are similar with both having a large −/+ (with increasing λ) couplet in the far UV and a weak negative band in the near UV, 260–300 nm region, as are compared in Figure 4 (dash-dot red and solid black lines, respectively). This same spectral pattern arises because W2W11 and W4W9 each have indole moieties about the same distance apart with the same relative angle of 80–90°, i.e. the rings are almost perpendicular.

The case of W2W9 is different (Fig. 4, green dash line). Two interesting features of the calculated spectra are the smaller ^{1}B intensities in the far-UV CD, which are also shifted to shorter wavelengths, and the positive CD computed for the near-UV ^{1}L band. The distance between the indole rings in W2W9 is 7 Å, but the angle between the planes is ~50°, and the overlap is offset, being largest between the five member rings on each indole rather than from the 6-member ring edge to the five member ring face as seen in W2W11 or W4W9. As a crude test of geometry sensitivity, we varied the angle between the indole planes in W4W9 to 74° and 52°. This showed the CD intensity and even its sign pattern to be quite angle sensitive. For the far separated Trp pair, W4W11, the computed ECD was very weak with the ^{1}B transition shifted up in energy,

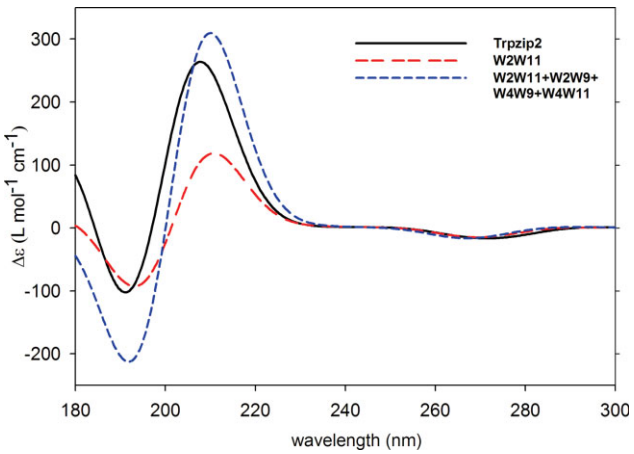

Fig. 5. Comparison of the calculated CD spectra for two (W2W11, red, dashed line) and four tryptophans (Trpzip2, black, solid line), and the summation of all four of the double mutant calculations (W2W11+W2W9+W4W9+W4W11, blue, short-dashed line). Calculations were performed on 3MI molecules constrained to the Trpzip2 geometry at the B3LYP/6-31G** level (smaller basis set results in a blue shift as compared to Fig. 4). [Color figure can be viewed in the online issue, which is available at www.interscience.wiley.com.]

reflecting the monomer value. Separated by 17 Å, these indoles couple only weakly, so that transition energies are roughly equivalent to the indole values and little CD is computed.

Trpzip2: Four Coupled Indoles Model

Finally, CD resulting from interactions of all four Trp side-chains in the Trpzip2 NMR structure were simulated using four 3MI molecules, oriented as shown in Figure 1. The resulting geometry was used to calculate CD with Turbomole 5.10 (which facilitated calculations on larger systems), and the molecule was modeled in vacuum with a smaller basis set for added computational stability and efficiency. To compare these four Trp results more directly to the two Trp containing cases (Fig. 4) we recalculated the spectra for the W2W11, W4W9, W2W9, and W4W11 pairs of indoles, this time also using Turbomole (B3LYP/6-31G**) and the vacuum approximation for consistency. Figure 5 shows the computed CD for four indoles interacting in the Trpzip2 geometry (solid black curve) as compared with that for just one pair (W2W11, red long-dashed curve) and for the sum of the four pairs (blue short-dashed curve), each computed independently. The main features of the full four indole case are similar to those of the two indole W2W11 case, namely a weak negative band in the 260–300 nm region and intense ^{1}B transitions forming a positive CD couplet in the far UV.

The computed bands are shifted up in frequency from those in Figure 4, due to the lack of solvent and diffuse functions (see Table 1) and the sum of the four pairs has a larger intensity, particularly in the negative ^1B_b band, than does the full calculation. The ^1L bands in both cases have similar intensity negative CD, which might not be expected by simply adding the spectra in Figure 4. The W2W9 contribution in Trpzip2 must cancel some of the negative CD from the ^1L transitions in W2W11 and W4W9, which explains the near agreement of the near UV CD (260–280 nm) for all three spectra in Figure 5. On the other hand, the ^{1}B CD in the far UV is much stronger in the Trpzip case as all the indole ^1B couplets have the same sign, so the contributions of the various pairs tend to add up. The resulting couplet shape is however different, being less conservative, since the lower energy positive band for four indoles is ~2.5 times more intense than for W2W11 and shifted up in energy, while the higher energy negative band is only slightly more intense, but again is also higher in energy for Trpzip2. This is not the same as the addition of four pairs overlapping as can be seen by comparing the CD of the sum of pairs (blue) with the Trpzip2 (four indole, solid) case, but that sum does have a smaller negative than positive lobe for the ^1B_b couplet. There is a positive CD band computed at ~180 nm, which may be seen here due to a different cutoff in the excited state computations for four indoles, which could contribute to the lower intensity for the high frequency (low wavelength) component.

DISCUSSION

Trpzip2 CD

Tryptophan residues provide important probes of structure for various spectroscopic techniques including UV absorbance, fluorescence, IR, Raman and CD. In this work we have probed a set of structures and their electronic transitions that give rise to the characteristic ECD bands for coupled Trp side-chains. Our study has taken a somewhat focused point of view in using just the Trp side-chain geometries from a set of tryptophan zipper molecules because it was originally targeted at explaining a specific chiroptical observation, the large couplet CD in the far UV spectra of the Trpzip peptides. This was of interest, since the CD of these is available in the literature and has been an important part of using chirality to understand the peptide folding mechanisms for modeling β-structure formation mediated by hydrophobic collapse.

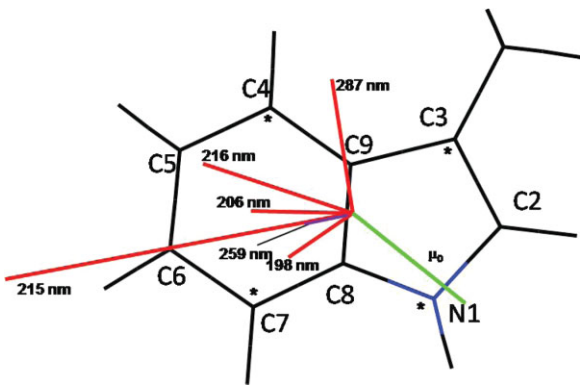

Fig. 6. Calculated (B3LYP/6-311++G**) permanent (green, $|\mu_0|$ = 2.02 debye) and in plane transition dipole moments (red) for 3MI that were used in the TDC computations (z-polarized transitions are not shown, further detail given in Supporting Information Table S3). The dipoles were placed in the geometrical center of the atoms marked by the asterisk. [Color figure can be viewed in the online issue, which is available at www.interscience.wiley.com.]

Our calculations initiated by focusing on a single indole, and extended to a methyl substituted indole to develop understanding of the impact of our computational schemes on the basic electronic $\pi-\pi^*$ transitions and their spectral properties. Once established, we computed spectra for two coupled indoles constrained to various conformations found in Trpzip2 and finally we considered all four indole side-chains corresponding to the full Trpzip2 structure, all computed at a TD-DFT level.

While this approach was, of course, designed to refine our methods and provide an interpretive basis for the final model calculation results, it also has a firm relationship to experimental results. We and others have synthesized series of related Trpzip peptides with varying numbers of Trp residues for the purpose of developing improved understanding of aromatic vs. hydrophobic interactions in stabilizing these hairpin structures. In particular we have previously prepared and discussed CD and IR spectra for a series of mutated Trpzip2 and Trpzip1 molecules that are substituted by either Val or Tyr for Trp to create structures with the substitution patterns represented here as W2W11 and W4W9.[4,5] [W2W9 and W4W11 were also synthesized in various forms, but neither formed a stable hairpin, thus we have no direct experimental CD data to compare to those calculations.]

Data from all these mutated Trpzip hairpins (some of which is reproduced in Figure 4b for Trpzip1 with various Tyr substitutions) showed the same qualitative patterns, four interacting Trp side-chains in each case had far-UV CD positive couplet that was much more intense than was the positive couplet for two interacting side-chains. All of these Trp containing, folded peptides gave the same couplet pattern in their far UV-CD, with a positive band lower in energy and more intense than the high frequency negative band. The quantitative aspects did vary depending on Tyr or Val substitution and did depend on the basic structure used, Trpzip2 or Trpzip1, but the qualitative pattern was consistent.

After convolving the overlapped TD-DFT transitions, the calculated magnitudes of the envelopes are in good agreement for W2W11 with the observed spectra (compare Fig. 4a and 4b) with a peak to peak $\Delta\epsilon$ of $\sim$209 (L mol^{-1} cm^{-1}) for the vacuum calculations, $\sim$141 for the PCM corrected ones and $\sim$148 for the experiment. These values more than double for the Trpzip2 (four Trps) structure, as are compared in Figure 5 and Supporting Information Table S4. Obviously these values are very sensitive to bandwidths chosen, but the overall agreement is clear. Since the difference in the far UV CD between four and two Trps in a hairpin was greater than 2, both theoretically and experimentally, simple additivity was insufficient to explain the observed exciton chirality.

Where measured, the ^1L transition in the near UV gave a negative weak CD that has some structure and collapsed upon unfolding with the same thermal behavior as characterized the collapse of the far-UV couplet at high temperatures.[6] As shown in Fig. 4c (in this case for Trpzip2), the ^1L_a, ^1L_b transitions yield negative CD of about $\Delta\varepsilon = -8.5$ (L mol^{-1} cm^{-1}) and in vacuum calculations are computed to overlap to yield $\Delta\epsilon$ approximately -16 (Figs. 4a and 5), again in acceptable agreement. With solvent correction, these computed values for the ^1L transitions fall by about half, somewhat more change than for the ^1B_b couplet. Taking the thermal dependence into account, both CD signals arise from coupling of Trp residues in a tertiary interaction.

The TD-DFT calculations presented here confirm the origin of these observed CD in the coupling of the indole side-chains of Trp. They further show that the W2W11 and W4W9 coupled CD should be similar and overlapping in frequency, both being more intense than the W2W9 CD. However computations indicate that the latter should not be particularly weak, which provides evidence that the W2W9 peptide studied experimentally lacks CD due to its being unfolded (disordered) and that its CD is not due to a lack of side-chain interaction (if the folded W2W9 conformation were maintained). This also provides an explanation of why the experimental Trpzip2 or Trpzip1 CD spectra are more than twice as intense as that of either W2W11 or W4W9 (see Fig. 4). In the stable folded Trpzip2 or Trpzip1, the W2W9 interaction would contribute with the same sign to the far UV CD but with a weaker couplet shifted to higher frequency. This interaction contributes to the Trpzip2 intensity, resulting in more than a doubling over the two-Trp case, but also tends to make the shape less symmetric, have a broader and weaker high frequency negative component, which is seen in our four-Trp calculations (Fig. 5) and is consistent with that observed experimentally. Our calculations do indicate that the long range W4W11 interaction has negligible contribution to the observed CD, even for the fully folded Trpzip2.

By contrast, the near UV situation is more complex, the W2W11 and W4W9 both have low energy negative contributions but the W2W9 interaction has the opposite sign due to the change in relative orientation of the two rings. This explains why the computed negative CDs for the four indole case and the two indole case (W2W11) are of comparable intensity in some of our calcuations (Fig. 5). However they do remain quite sensitive to basis set and solvation model.

Ring orientation is the basic structural parameter explored by exciton coupled CD. In this case we have done selected test calculations with rings held at alternate angles and obtained CD that changed in amplitude and even in sign. These computations are difficult to quantify, since variation in relative twist of the rings as well as interplanar angle can change the coupling and was not independently controlled.

We analyzed the Kohn-Sham orbitals to interpret the basic features of the states contributing to the CD spectra. The negative band in the 270–300 nm region is due to the ^1L_a $\pi-\pi^*$ transition, as would be seen in polar solvents (modeled here implicitly), and ^1L_a is more intense than ^1L_b. Although the experimental ^1L_a may have fine structure, this would not be seen in our calculated spectra which do not include any vibronic coupling.[23] The negative–positive couplet in the 190–230 nm region can be interpreted in terms of coupling of the ^1B_b transitions on each indole.[23] These are $\pi-\pi^*$ transitions from the HOMO and HOMO-1 to higher unoccupied orbitals.

Because of coupling, the rotational strengths for the ^1B transitions are calculated to be an order of magnitude more intense than for the ^1L transitions. For a single indole, even if it were in a chiral environment, the ^1B_b would give a quite weak CD response, although the ^1L transitions do couple to their environment and yield diagnostically useful CD.[7]

It is important to recognize that these calculations primarily have a qualitative value. In this case the frequencies observed for the near- and far-UV transitions are in exceptionally good agreement with the calculational results but the quantitative aspects are quite dependent on the basis set and functional used as well as band widths used in the spectral simulation (see Table 1). The former is especially evident in comparing the computed spectra in Figure 4, where W2W11 has a positive band at 235 nm, with those in Figure 5, where this positive band in W2W11 appears at 212 nm. The later was calculated for a molecule in vacuum with a simpler polarized basis set, while the former is corrected for solvent (PCM) and used a diffuse basis set. Experimentally these transitions are found at ~227 (+) and ~213 (−) nm in Trpzip2 and W2W11 and W4W9, suggesting the 6-31++G**/PCM approach is a much better choice.

The qualitative pattern for the far-UV exciton coupled CD can also be modeled using semiclassical TDC for the component splitting and CO methods for their rotational strengths. As has been noted by others, the strong ^1B_b transition has a dipole moment located along the long axis (passing through C2 and bisecting the bond between C5 and C6) of the indole moiety and the ^1L_a and ^1L_b transition dipoles are oriented roughly 45° off that direction (see Fig. 6).[12,13,25] To model this interaction more completely, we chose a multidipole coupling method, as summarized earlier in the "Methods" section, making use of our TD-DFT computed dipole moments for the indole (3MI) monomer transitions. This classically modeled far UV CD provided the same qualitative sign pattern for W2W11 and W4W9 as well as for Trpzip2, which is shown in the Supporting Information Figure S1. The near-UV CD of the ^1L transitions is computed to be weak in the TDC-CO model, particularly with respect to the ^1B_b transition couplet, and change by about a factor of two from W2W11 to Trpzip2, but still comparable to our experimentally observed value.[6] On the other hand the ^1B couplet results with the TDC-CO model yield CD bands about twice as intense as those calculated with the TD-DFT method and similarly much larger than seen experimentally, particularly for the four-Trp, Trpzip2 model (see comparison, Supporting Information Table S4). This may be due to different dispersion with just dipole coupling or to other factors. However it is clear that the couplet results primarily from coupling of the ^1B transition dipole on each chromophore through the characteristic Trpzip2 edge-to-face indole geometry. If the angles are distorted from perpendicular, the CD magnitudes decrease.

CONCLUSIONS

The electronic CD of tryptophan side-chains in a Trpzip peptide was modeled by TD-DFT calculations for alkyl substituted indole rings. For a pair of indoles, the CD in the far-UV region, 190–230 nm, arises from coupling of the $\pi-\pi^*$ ^1B_b transitions, which arise primarily from the HOMO, HOMO-1 to LUMO+1 and the LUMO+2 transitions. The simulated CD reproduces the intense negative–positive couplet in the far UV and the negative band in the near-UV region that are observed experimentally. This confirms that the intense far-UV CD in Trp-rich beta hairpins such as Trpzip are dominated by interactions of the Trp sidechain transitions without a significant contribution from the amide backbone transitions. Simpler dipole coupling models provide a similar qualitative picture for the electric dipole allowed ^1B_b transitions, but magnitudes are not as directly comparable to the experiment and the CD arising from the ^1L_a and ^1L_b transitions are not predicted well with such classical models.

ACKNOWLEDGMENTS

The authors thank Ling Wu and Dan McElheny for discussion of their NMR structural results for the Trpzip peptides, and Ling Wu, Rong Huang, and Takahiro Takekiyo for access to their experimental CD spectra before publication.

LITERATURE CITED

1. Cochran AG, Skelton NJ, Starovasnik MA. Tryptophan zippers: stable, monomeric β-hairpins. Proc Natl Acad Sci USA 2001;98:5578–5583.
2. Tatko CD, Waters ML. Selective aromatic interactions in beta-hairpin peptides. J Am Chem Soc 2002;124:9372–9373.
3. Cochran AG, Skelton NJ, Starovasnik MA. Correction. Proc Natl Acad Sci USA 2002;99:9081–9081.
4. Wu L, McElheny D, Huang R, Keiderling TA. Role of Trp-Trp interactions in a Trpzip β-hairpin formation, structure and stability. Biochemistry; 2009; in press.
5. Takekiyo T, Wu L, Yoshimura Y, Shimizu A, Keiderling TA. Relationship between hydrophobic interactions and secondary structure stability for Trpzip β-hairpin peptides. Biochemistry 2009;48: 1543–1552.
6. Huang R, Wu L, McElheny D, Bour P, Roy A, Keiderling TA. Cross-strand coupling and site-specific unfolding thermodynamics of a Trpzip β-hairpin peptide using 13C isotopic labeling and IR spectroscopy. J Phys Chem B 2009;113:5661–5674.
7. Hauser K, Krejtschi C, Huang R, Wu L, Keiderling TA. Site-specific relaxation kinetics of a tryptophan zipper hairpin peptide using temperature-jump IR spectroscopy and isotopic labeling. J Am Chem Soc 2008;130:2984–2992.
8. Rogers DM, Besley NA, O'Shea P, Hirst JD. Modeling the absorption spectrum of tryptophan in proteins. J Phys Chem B 2005;109:23061–23069.
9. Dedonder-Lardeux C, Jouvet C, Perun S, Sobolewski AL. External electric field effect on the lowest excited states of indole: ab initio and molecular dynamics study. Phys Chem Chem Phys 2003;5:5118–5126.
10. Platt JR. Classification of spectra of cata-condensed hydrocarbons. J Chem Phys 1949;17:484–495.
11. Vivian JT, Callis PR. Mechanisms of tryptophan fluorescence shifts in proteins. Biophys J 2001;80:2093–2109.
12. Robinson D, Besley NA, Lunt EAM, O'Shea P, Hirst JD. Electronic structure of 5-hydroxyindole: from gas phase to explicit solvation. J Phys Chem B 2009;113:2535–2541.
13. Slater LS, Callis PR. Molecular-orbital theory of the ^1L_a and ^1L_b states of indole.2. an ab-initio study. J Phys Chem 1995;99:8572–8581.
14. Grishina IB, Woody RW. Contributions of tryptophan side chains to the circular dichroism of globular proteins: exciton couplets and coupled oscillators. Faraday Discuss 1994;4:245–262.

15. Grimme S, Parac M. Substantial errors from time-dependent density functional theory for the calculation of excited states of large pi systems. Chem Phys Chem 2003;4:292–295.
16. Sebek J, Bour P. Ab initio modeling of the electronic circular dichroism induced in porphyrin chromophores. J Phys Chem A 2008;112: 2920–2929.
17. Mennucci B, Tomasi J. Continuum solvation models: A new approach to the problem of solute's charge distribution and cavity boundaries. J Chem Phys 1997;106:5151–5158.
18. Frisch MJ, T GW, Schlegel HB, Scuseria GE, Robb MA, Cheeseman JR, Montgomery JA Jr., Vreven T, Kudin KN, Burant JC, Millam JM, Iyengar SS, Tomasi J, Barone V, Mennucci B, Cossi M, Scalmani G, Rega N, Petersson GA, Nakatsuji H, Hada M, Ehara M, Toyota K, Fukuda R, Hasegawa J, Ishida M, Nakajima T, Honda Y, Kitao O, Nakai H, Klene M, Li X, Knox JE, Hratchian HP, Cross JB, Bakken V, Adamo C, Jaramillo J, Gomperts R, Stratmann RE, Yazyev O, Austin AJ, Cammi R, Pomelli C, Ochterski JW, Ayala PY, Morokuma K, Voth GA, Salvador P, Dannenberg JJ, Zakrzewski VG, Dapprich S, Daniels AD, Strain MC, Farkas O, Malick DK, Rabuck AD, Raghavachari K, Foresman JB, Ortiz JV, Cui Q, Baboul AG, Clifford S, Cioslowski J, Stefanov BB, Liu G, Liashenko A, Piskorz P, Komaromi I, Martin RL, Fox DJ, Keith T, Al-Laham MA, Peng CY, Nanayakkara A, Challacombe M, Gill PMW, Johnson B, Chen W, Wong MW, Gonzalez C, Pople JA. Gaussian 03, Revision D.02, Wallingford CT: Gaussian, Inc.; 2004.
19. TURBOMOLE V5.10 2009, a development of University of Karlsruhe and Forschungszentrum Karlsruhe GmbH, 1989–2007, TURBOMOLE GmbH, since 2007. Available at http://www.turbomole.com.
20. Zhong W, Gulotta M, Goss DJ, Diem M. DNA solution conformation via infrared circular dichroism: experimental and theoretical results for B-family polymers. Biochemistry 1990;29:7485–7491.
21. Charney E. The molecular basis of optical activity. New York: Wiley; 1979.
22. Rogers DM, Hirst JD. First-principles calculations of protein circular dichroism in the near ultraviolet. Biochemistry 2004;43:11092–11102.
23. Tomasvert F, Ponce CA, Estrada MR, Silber J, Singh J, Anunciatta J. Experimental and theoretical-studies on the electronic-spectra of indole-3-acetic-acid and its anionic and protonated species. J Mol Struct 1991;246:203–215.
24. Pescitelli G, Di Bari L, Caporusso AM, Salvadori P. The prediction of the circular dichroism of the benzene chromophore: TDDFT calculations and sector rules. Chirality 2008;20:393–399.
25. Albinsson B, Norden B. Excited-state properties of the indole chromophore: electronic transition moment directions from linear dichroism measurements: effect of methyl and methoxy substituents. J Phys Chem 1992;96:6204–6212.